COMPUTATIONAL MECHANICS 2021
36th conference with international participation
Srní
November 8 - 10, 2021

Electrolyte flow through piezoelectric porous media and its application to two-scale cortical bone modeling

J. Camprová Turjanicová[a,b], E. Rohan[a,b]

[a] *Faculty of Applied Sciences, University of West Bohemia, Univerzitní 8, 301 00 Plzeň, Czech Republic*
[b] *NTIS – New Technologies for the Information Society, Univerzitní 8, 301 00 Plzeň, Czech Republic*

In biomechanics, electrochemical interactions between ions and negatively charged surfaces of the porous material occur in a few types of biological tissues. Our interest lies in the modeling of the cortical bone porous structure, where the transport of the ions in the proximity of charged collagen-apatite matrix has shown to play a role in bone regrowth and remodeling. Upon stress, bone tissue generates an electrical potential that directly influences the activity of bone cells. With this in mind, we derive the model of electrolyte flow through piezoelectric porous media and apply it to simulate the processes in cortical bone.

The cortical bone is a strictly hierarchical system with a complicated porous structure on different scale levels. The cortical bone tissue comprises a system of approximately cylindrical sub-units called osteons, see Fig. 1. Each osteon has a radius of approximately 100-150 μm, [5], with a hollow canal in its center. It is called the Haversian canal (HC) and contains blood vessels and nerves with rest of the space occupied by the bone fluid. The walls of the HC are covered by bone cells. Behind this bone cell layer, the walls of the HC are perforated by a network of small interconnected channels known as canaliculi, [5]. The canaliculi network connects the HC and lacunae, which are ellipsoidal cavities containing one bone-creating cell each, i.e., an osteocyte. The lacunar-canalicular network (LCN) is also saturated by bone fluid that transports nutrients and information about mechanical loading.

The cortical bone consists of two phases at the microscopic scale: the collagen-hydroxyapatite matrix and the bone fluid that fills the LCN. For modeling, we imagine the bone fluid as a salt-

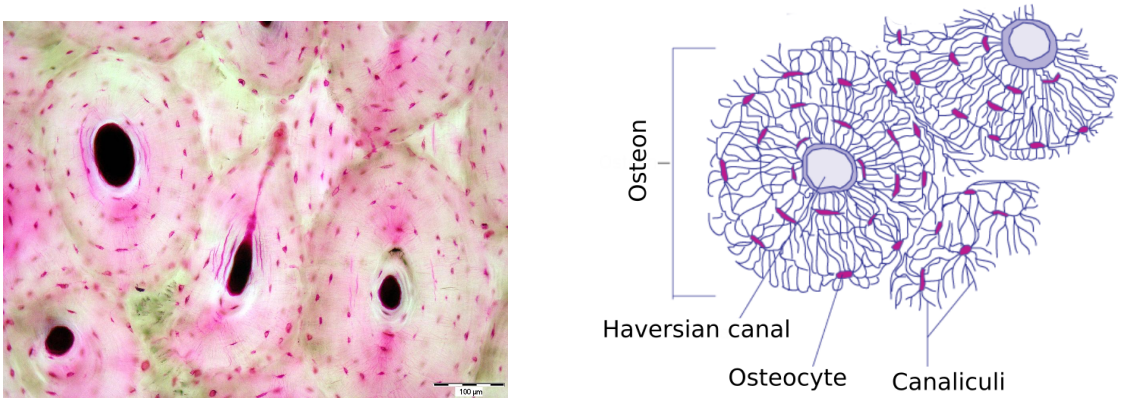

Fig. 1. Cortical bone structure: (*left*) the osteonal structure in cortical bone tissue, scale of 100 μm; (*right*) the illustration of lacunar-canalicunar network in the osteonal structure

water solution. Thus, there are two types of ions (further indexed by $\alpha = 1, 2$) with opposite polarization and that are defined by their respective diffusivity coefficients D_α^0. The bone fluid is an incompressible Newtonian fluid characterized by dynamic viscosity η_f.

Due to the presence of collagen, the bone matrix is deformable. Moreover, it exhibits piezoelectric behavior that was first reported by [2]. Biopolymers, such as collagen-hydroxyapatite, usually have the specific symmetry type: the piezoelectric coupling tensor $\boldsymbol{g}$ and dielectric tensor $\boldsymbol{d}$ are defined by their components g_{14}, $g_{25} = -g_{14}$, and d_{11}, $d_{22} = d_{11}$, d_{33}. Elastic properties of this type of material are transversal isotropic with the elastic tensor characterized by Young's moduli E_1, E_3, shear modulus G_{13} and Poisson's ratios ν_{12}, ν_{31}, [3].

The modeling of cortical bone tissue presents a unique challenge because of its highly hierarchical structure and complex interaction between phases. To simulate such material by direct modeling of its whole microstructure in its complexity would be very taxing on the computational memory requirements and not practical for bigger and more complex simulations. Instead, the material's heterogeneity is dealt with by applying a suitable homogenization method, such as unfolding homogenization (UFH). The UFM also respects the microstructure of the porous medium and, through the introduction of scale separation formulae, provides us with tools to reconstruct the macroscopic solution on the microscopic scale.

To successfully apply the UFH, we assume that the cortical bone tissue occupies domain Ω. The domain Ω is decomposed into solid and fluid phase, Ω_s and Ω_f, that have designated parts of the external boundary, $\partial_{\text{ext}}\Omega_s$ and $\partial_{\text{ext}}\Omega_f$, and interface $\Gamma = \partial\Omega_s \cup \partial\Omega_f$. Domain Ω is generated by periodical repeating copies of representative volume element (RVE) Y scale by ε. The RVE Y is decomposed into solid and fluid phase, Y_s and Y_f, with interface $\Gamma_Y = \bar{Y}_s \cup \bar{Y}_f$.

The homogenization procedure yields the expressions for computing the effective tensors that describe the behavior at the macroscopic scale. The tensors relevant to the ionic transport are tensor of permeability $\boldsymbol{\mathcal{K}}$, migration-diffusion tensors $\boldsymbol{\mathcal{J}}^\beta$, Onsager tensors $\boldsymbol{\mathcal{L}}^\beta$, diffusivity tensors $\boldsymbol{\mathcal{D}}^{\alpha\beta}$ and two new tensors $\boldsymbol{\mathcal{Q}}^{\alpha\beta}$ and $\boldsymbol{\mathcal{S}}^{\alpha\beta}$. Further, it gives tensors related to the piezoelectricity, which are piezoelasticity tensor $\boldsymbol{\mathcal{A}}$, modified Biot's tensor $\boldsymbol{\mathcal{B}}$, and ionic potential tensor $\boldsymbol{\mathcal{C}}^\alpha$. Then, the dimensionless macroscopic homogenized system of equations, where the external electrical field is omitted, reads: Find global pressure P^0, displacement $\boldsymbol{u}^0$ and ionic potentials $\Phi_\alpha^0, \alpha = 1, 2$, such that

$$
\begin{aligned}
\nabla_x \cdot \left[\boldsymbol{\mathcal{K}}(\boldsymbol{f} - \nabla_x P^0) + \sum_{\beta=1}^{2} \boldsymbol{\mathcal{J}}^\beta \nabla_x \Phi_\beta^0 \right] + \mathcal{M}\partial_t P^0 - \boldsymbol{\mathcal{B}} : e_x\left(\partial_t \boldsymbol{u}^0\right) - \mathcal{N}^\beta \partial_t \Phi_\beta^0 = 0, \\
\sum_{\beta=1}^{2} (\boldsymbol{\mathcal{Q}}^{\alpha\beta} + \boldsymbol{\mathcal{S}}^{\alpha\beta}) \partial_t \Phi_\beta^0 + \nabla_x \cdot \left[\boldsymbol{\mathcal{L}}^\alpha(\boldsymbol{f} - \nabla_x P^0) + \sum_{\beta=1}^{2} \boldsymbol{\mathcal{D}}^{\alpha\beta} \nabla_x \Phi_\beta^0 \right] = 0, \qquad (1) \\
-\nabla_x \cdot \boldsymbol{\mathcal{A}} e_x\left(\boldsymbol{u}^0\right) + \nabla_x \cdot \left[\boldsymbol{\mathcal{B}} P^0 - \sum_{\beta=1}^{2} \boldsymbol{\mathcal{C}}^\alpha \Phi_\beta^0 \right] = \boldsymbol{f}
\end{aligned}
$$

for $\alpha = 1, 2$ and completed by boundary conditions given below. We can distinguish the fluid seepage velocity $\boldsymbol{w}^0$, the ionic diffusion fluxes $\boldsymbol{j}_\alpha^0, \alpha = 1, 2$, and the porous body stress $\boldsymbol{\sigma}^0$,

$$
\begin{aligned}
\boldsymbol{w}^0 &= \sum_\beta \boldsymbol{\mathcal{J}}_\beta \nabla_x \Phi_\beta^0 - \boldsymbol{\mathcal{K}}(\nabla_x P^0 - \boldsymbol{f}) \quad \text{in } \Omega, \\
\boldsymbol{\sigma}^0 &= \boldsymbol{\mathcal{A}} e_x(\boldsymbol{u}^0) - P^0 \hat{\boldsymbol{\mathcal{B}}} + \sum_\beta \boldsymbol{\mathcal{C}}^\beta \Phi_\beta^0 \quad \text{in } \Omega, \qquad (2) \\
\boldsymbol{j}_\alpha^0 &= \sum_\beta \boldsymbol{\mathcal{D}}_{\alpha\beta} \nabla_x \Phi_\beta^0 - \boldsymbol{\mathcal{L}}_\alpha(\nabla_x P^0 - \boldsymbol{f}) \quad \text{in } \Omega, \quad \alpha = 1, 2.
\end{aligned}
$$

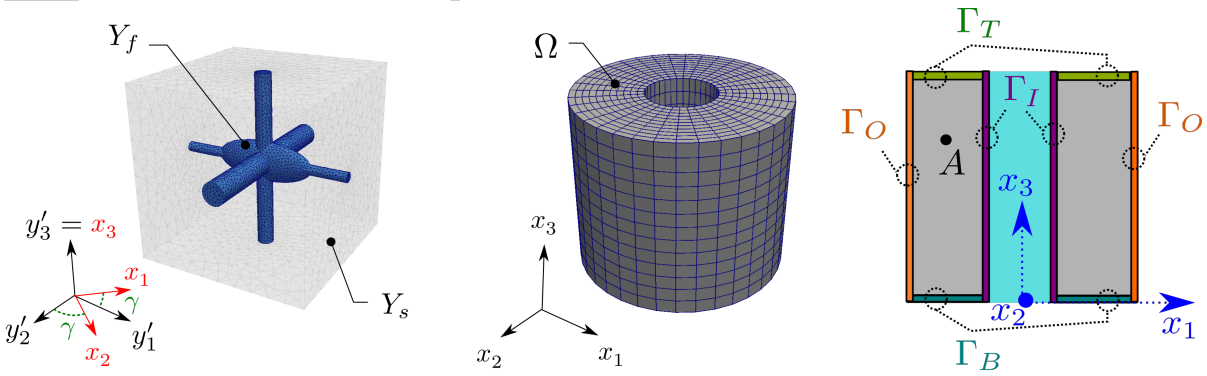

(a) (b) (c)

Fig. 2. (a) Mesh representation of RVE Y; (b) mesh representation of single bone osteon, i.e., domain Ω; (c) definition of boundaries of domain Ω

The system (1) needs to be completed by a set of boundary conditions given below.

For numerical modeling, we simplify the bone structure into two structural levels and propose their geometry representation, as follows:

- The microscopic level represents the LCN filled with bone fluid. The cubic RVE Y represents three channels with a single ellipsoidal lacuna, see Fig. 2a. The three channels have a cross-sectional area corresponding to the sum of cross-sectional areas of all the canaliculi in the given direction to preserve the flow rate between lacunae, [1].
- The macroscopic level is represented by a single osteon which has an approximately cylindrical shape with a hollow canal in its center, see Fig. 2b.

To respect the orientation of LCN in osteon, the computed effective coefficients are circumferentially rotated around the x_3-axis of the central canal.

We consider the inner osteonal wall Γ_I to be non-permeable. The gradual compression is applied at the top of the osteon, i.e., at Γ_T. This is realized through the following boundary value problem (BVP), which is defined by (1) and by the boundary conditions of Neumann and Dirichlet type. The boundary conditions are applied to the parts of macroscopic specimen boundary, in the following manner (for all $t \in]0, T[$):

- $u_1 = u_2 = 0, \quad u_3(t) = \bar{u}(t)t, \quad \boldsymbol{n} \cdot \boldsymbol{j}_\alpha = 0, \quad \boldsymbol{n} \cdot \boldsymbol{w} = 0$ on Γ_T,
- $\boldsymbol{u}(t) = \boldsymbol{0}, \quad \boldsymbol{n} \cdot \boldsymbol{j}_\alpha = 0, \quad \boldsymbol{n} \cdot \boldsymbol{w} = 0$ on Γ_B,
- $\boldsymbol{n} \cdot \boldsymbol{j}_\alpha = 0, \quad \boldsymbol{n} \cdot \boldsymbol{w} = 0, \quad \boldsymbol{n} \cdot \boldsymbol{\sigma}_s^p = 0$ on Γ_O,
- $P = \bar{P}, \quad \Phi_1 = \bar{\Phi}_1, \quad \Phi_2 = \bar{\Phi}_2, \quad \boldsymbol{n} \cdot \boldsymbol{\sigma}_s^p = 0$ on Γ_I,

where $\boldsymbol{\sigma}, \boldsymbol{w}$ and $\boldsymbol{j}_\alpha, \alpha = 1, 2$, are given by (2) and $\bar{u}(t) = 0.1t$. The prescribed values of boundary conditions are $\bar{P} = 1.0, \bar{\Phi}_1 = -0.01, \bar{\Phi}_2 = 0.01$.

Initial conditions are taken from the steady-state solution (i.e., for $t = 0$) of the macroscopic problem (1) with a set of boundary conditions given above. The numerical implementation of the homogenized model completed by suitable choice of initial and boundary conditions was made in python-based FEM software *SfePy*. Let us note that the macroscopic problem is solved in its dimensionless form. However, its results can be easily dimensionalized. Thus, all the following results are in dimensionalized form denoted by $\sqcup^{\text{eff}}$.

All the presented results are axially symmetric, which is the direct consequence of the circumferential orientation of the microstructure in the macroscopic specimen. Thus, Fig. 3 shows the distribution of macroscopic solution $(p^{\text{eff}}, \boldsymbol{u}^{\text{eff}}, \Phi_\alpha^{\text{eff}})$, $\alpha = 1, 2$, of BVP at $t = T$ along the radial axis that passes through the point A, see Fig. 2c.

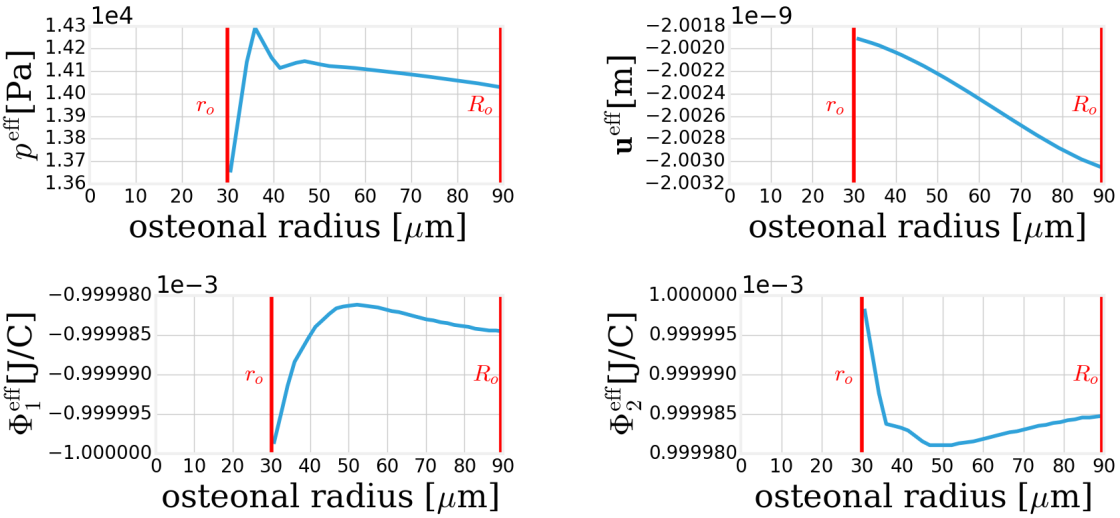

Fig. 3. BVP IV: Distribution of macroscopic fields $(p^{\text{eff}}, \boldsymbol{u}^{\text{eff}}, \Phi_\alpha^{\text{eff}})$, $\alpha = 1, 2$, at $t = T$ along the radial axis. The values of radius of HC r_o and radius of osteon R_0 are denoted by red vertical lines

The presented model computational model can be used not only for studying processes in the cortical bone but also for a wide range of other applications due to the derivation of equations in general dimensionless form. The chosen homogenization method also enables us to study the effect of the macroscopic fields on the microscale. This work is the extension of our previous research, so we refer to it for more details, [4].

Acknowledgements

The work was supported in part by the project GACR 19-04956S of the Scientific Foundation of the Czech Republic, by the European Regional Development Fund-Project "Application of Modern Technologies in Medicine and Industry" (No. CZ.02.1.01/0.0/0.0/17 048/0007280), and the project SGS-2019-002.

References

[1] Beno, T., Yoon, Y.J., Cowin, S.C., Fritton, S.P., Estimation of bone permeability using accurate microstructural measurements, Journal of biomechanics 39 (13) (2006) 2378-2387.

[2] Fukada, E., Yasuda, I., On the piezoelectric effect of bone, Journal of the Physical Society of Japan 12 (10) (1957) 1158-1162.

[3] Silva, C., Thomazini, D., Pinheiro, A., Aranha, N., Figueiro, S., Góes, J., Sombra, A., Collagen–hydroxyapatite films: Piezoelectric properties, Materials Science and Engineering: B 86 (3) (2001) 210-218.

[4] Turjanicová, J., Rohan, E., Lukeš, V., Homogenization based two-scale modelling of ionic transport in fluid saturated deformable porous media, Computers & Mathematics with Applications 78 (9) (2019) 3211-3235.

[5] Yoon, Y. J., Cowin, S. C., The estimated elastic constants for a single bone osteonal lamella, Biomechanics and Modeling in Mechanobiology 7 (1) (2008) 1-11.